

# Design of Fir Digital Bandpass Filter with Hamming Window and Hanning Window Method for Fetal Doppler

Hartono Siswono, Widyastuti Suwandi, Yohanes Dovan, Dyah Nur'ainingsih

Department of Electrical Engineering, University of Gunadarma, Jl. Margonda Raya no 100, Depok 16424, Indonesia

## ARTICLE INFO

### Article history:

Received August 02, 2023  
Revised September 13, 2023  
Published October 07, 2023

### Keywords:

Bandpass Filter;  
Fetal Heart Rate;  
Finite Impulse Response (FIR)  
Hamming Window;  
Hanning Window

## ABSTRACT

Fetal heart rate using Doppler Ultrasound is a standard method to assess fetal health. Examination of the fetal heart with a Doppler device is more convenient for women. Fetal Doppler can accidentally take the mother's heartbeat. A filter is needed to enhance the audibility of fetal heartbeats while suppressing unwanted frequencies and noise. The normal fetal heart rate ranges from 120 to 160 beats per minute, or 2 Hz - 3 Hz. This frequency can be filtered using a bandpass filter. The digital FIR bandpass filter were created using the Hamming and Hanning window methods. The results of the FIR filter with the Hamming and Hanning window, Orde 100 Hanning gave the best frequency bandwidth range which was 1.833 Hz to 3.167 Hz. Orde 20 Hamming and Hanning had the shortest delay  $\pm 2$  s and Orde 100 Hamming and Hanning had the longest delay  $\pm 6$  s. For the noise at 1.6 Hz, Orde 100 Hamming and Orde 100 Hanning the signal level of the signal output is the same as the desired signal level. For the noise at 3.1 Hz, Orde 100 Hamming and Orde 100 Hanning had the signal level of the signal output is almost the same as the desired signal level. At the frequency point of 1.6 Hz, the noise signal at the input has a magnitude response 2533, it is a decrease after passing through the filter to  $\approx 0$ . At the frequency point of 3.1 Hz, the noise signal at the input has a magnitude response 2246, and there is a decrease after passing through the filter to 167.7. From this study, we can choose 100 orde Hanning because it gave the best frequency bandwidth range which was 1.833 Hz to 3.167 Hz, the delay of  $\pm 6$  s.

This work is licensed under a [Creative Commons Attribution-Share Alike 4.0](https://creativecommons.org/licenses/by-sa/4.0/)



## Corresponding Author:

Hartono Siswono, Electrical Engineering, University of Gunadarma, Jl. Margonda Raya no 100, Depok 16424, Indonesia  
Email: [hartono@staff.gunadarma.ac.id](mailto:hartono@staff.gunadarma.ac.id)

## 1. INTRODUCTION

Fetal heart rate (FHR) monitoring using Doppler Ultrasound (US) is a standard method to assess fetal health before and during labor [1]-[6]. A filter is needed on the fetal doppler for the sound of the fetal heartbeat can be heard clearly. The normal fetal heart rate in the womb ranges 120 to 160 beats per minute [7]-[9], or 2 Hz - 3 Hz [10], [11].

Fetal doppler is a diagnostic tool that uses the doppler effect to simulate the sound of a fetal heartbeat. Examination of the fetal heart with a Doppler device is more convenient for women and the sound emitted can be heard by everyone present in the room including the pregnant woman, this is good for reassuring women and their families. Because of its sensitivity, fetal doppler can accidentally take the mother's heartbeat, and should be verified by feeling the mother's pulse simultaneously [12]-[15].

A filter is needed on the fetal doppler so that the sound of the fetal heartbeat can be heard clearly. The filter functions as a damper for unwanted components of a signal (noise), and passes the information component contained in the signal. The normal fetal heart rate in the womb ranges from 120-160 beats per minute or has a frequency range of 2 Hz - 3 Hz. To achieve precise fetal heartbeat audibility, effective filtering is indispensable. Filters act as dampers for extraneous signal components, including noise, while preserving the crucial information within the signal itself. Given the distinct frequency range of fetal heartbeats (2 Hz - 3 Hz), a bandpass filter proves valuable in isolating and amplifying this range while attenuating frequencies beyond it.

Consequently, the primary focus of this study is the design and evaluation of filters tailored to fetal Doppler devices. Specifically, we explore six filter configurations: 20-order Hamming Window, 50-order Hamming Window, 100-order Hamming Window, 20-order Hanning Window, 50-order Hanning Window, and 100-order Hanning Window [16]-[23]. The objective is to determine the optimal filter design that best enhances fetal heartbeat audibility and minimizes unwanted interference.

## 2. METHODS

### 2.1. Digital Filter

In signal processing, a filter is an essential tool for eliminating unwanted components from a signal, such as noise or undesired frequencies [24]-[26]. In the context of this study, the focus is on a digital bandpass filter, which selectively allows the signal to pass at a specific center frequency while attenuating frequencies below and above that range [27]-[29].

### 2.2. FIR Digital Filter

In the FIR filter, the impulse response,  $h(n)$ , is limited to a finite number. Impulse response can be stated by:

$$\begin{aligned} h(n) &= a_n \text{ for } 0 \leq n \leq k \\ &= 0 \text{ for others} \end{aligned} \quad (1)$$

with Transfer Function:

$$H(z) = \sum_{m=0}^k a_m z^{-m} \quad (2)$$

[30]-[34]

### 2.3. Fourier Series Method

The Fourier series approach is somewhat fundamental in that the other methods use the same theoretical basis. The Fourier series method is more straightforward in concept, hence will be used as a basis. One of the disadvantages is that it is not easy to pre-state the correct level for the ripple level in the passband and stopband. Therefore, it is necessary to investigate alternative designs to obtain a suitable function for the filter specifications. This method is best used with "window functions".

The response frequency is expressed in terms of normalized frequency  $v = f/f_0$ , where  $f_0 = fs/2$  is the folding frequency.  $A_d(v)$  is given as the amplitude of the desired response,  $A(v)$  is the normalized value.

Then the cosine series in  $A(v)$  and  $c_m$  is:

$$A(v) = \sum_{m=-M}^m c_m e^{jm\pi v} \quad (3)$$

$$c_m = \int_0^1 A_d(v) \cos m\pi v \, dv \quad (4)$$

[35]-[37]

### 2.4. Window Functions

If  $w_m$  represents the coefficient of the window function, and  $c_m'$  represents the coefficient of the modified transfer function, then:

$$c'_m = w_m c_m \quad (5)$$

Then the modified transfer function is expressed by:

$$H'_1(z) = \sum_{m=-M}^m c'_m z^{-m} \quad (6)$$

The end result is:

$$H(z) = \sum_{i=0}^M a_i z^{-i} \quad (7)$$

with

$$a_i = c'_{M-i} \quad (8)$$

In this paper, only two window functions are used, which are Hamming and Hanning Window. In Hamming Window

$$w(t) = 0.54 + 0.46 \cos \frac{2\pi t}{\tau} \text{ for } |t| < \frac{\tau}{2} \quad (9)$$

In Hanning Window

$$w(t) = \cos^2 \frac{\pi t}{\tau} = \frac{1}{2} \left( 1 + \cos \frac{2\pi t}{\tau} \right) \text{ for } |t| < \frac{\tau}{2} \quad (10)$$

[38]-[45]

## 2.5. Sampling Theorem

The sampling theorem, also known as Shannon's theorem or Kotelnikov's theorem, states that at the minimum rate any signal to be sampled so that it can be reconstructed from its sampled value, is twice the highest frequency component present in the signal.

$$f_s \geq 2f_m \quad (11)$$

[46]-[47]

If the  $f_s < 2f_m$ , it will give aliasing which is the overlapping of frequency components. This overlap results in distortion or artifacts when the signal is reconstructed from samples which causes the reconstructed signal to differ from the original continuous signal.

## 3. RESULTS AND DISCUSSION

Making FIR filters using the window function approach requires continuous testing until a filter order that meets the specifications is obtained, therefore, in this study there are 6 filters which are Hamming Window and Hanning Window with order 20, order 50, and order 100.

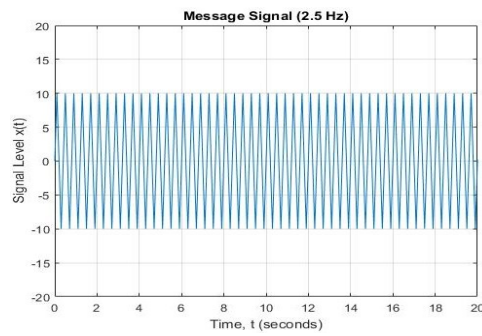
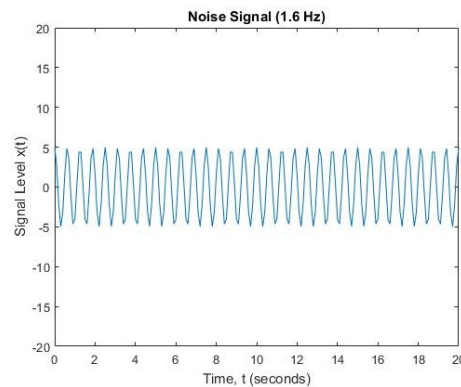
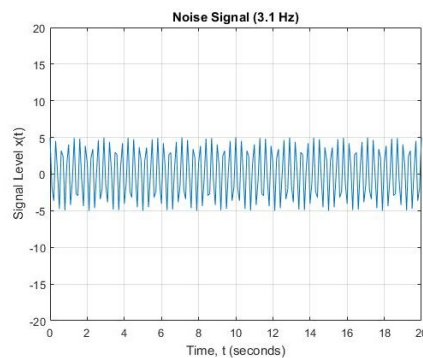
The required input to the FIR digital bandpass filter is the value of the sampling frequency. This value is obtained from the sampling process on the analog sound signal of the fetal heartbeat which has a frequency of 2 Hz – 3 Hz. The sampling frequency value must be at least twice the information frequency to operate on a digital signal processing system. Because of that, we need the sampling frequency must be greater than 6 Hz.

### 3.1. FIR Digital Bandpass Filter Design Specification

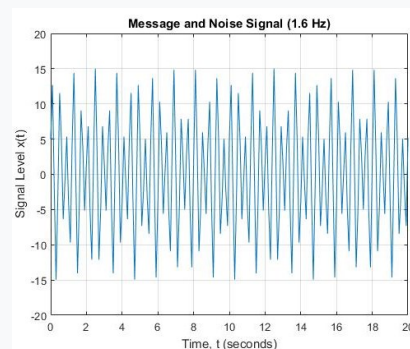
To achieve the desired filter characteristics, we designed six FIR filters using Hamming and Hanning Window methods with varying orders: 20, 50, and 100. The key objective was to assess the suitability of these filters for fetal Doppler signal processing. The FIR digital bandpass filter required the sampling frequency, determined by the fetal heartbeat frequency range of 2 Hz - 3 Hz, necessitating a sampling frequency greater than 6 Hz.

### 3.2. Generating Information Signals and Noise Signals

In the initial simulation step, we generated an information signal representing the fetal heart rate (2.5 Hz) and introduced noise signals (1.6 Hz and 3.1 Hz) to emulate real-world conditions (Fig. 1-Fig. 3). The simulation using MATLAB.

**Fig. 1.** Input Signal 2.5 Hz**Fig. 2.** Signal Noise 1.6 Hz**Fig. 3.** Signal Noise 3.1 Hz

These two noise signals are then added to the information signal to become an analog input signals (Fig 4-Fig. 5).

**Fig. 4.** 2.5 Hz Input Signal with 1.6 Hz Noise

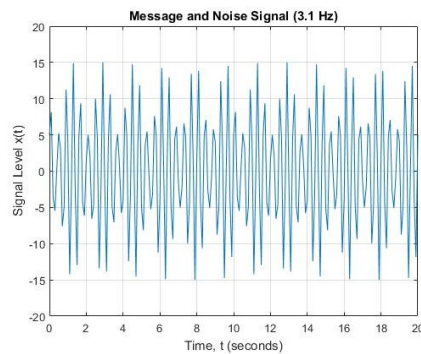


Fig. 5. 2.5 Hz Input Signal with 3.1 Hz Noise

### 3.3. FIR Orde 20 Digital Bandpass Filter Simulation

FIR Orde 20 digital bandpass filter simulation using Filter Designer which is part of the MATLAB software. The filter will be simulated with 2 different methods, the Hamming Window and the Hanning Window to see which method produces the best output signal.

Fig. 6(a) indicates that the frequency bandwidth range to be passed on the orde 20 FIR digital bandpass filter using the Hamming Window method still widens to 1.138 Hz – 3.862 Hz exceeding the bandwidth range that should be 2 Hz – 3 Hz, this indicates that orde 20 Hamming Window still does not meet the required specifications in Fig. 6(b). It is known that the frequency bandwidth range that will be passed on the 20th orde FIR Digital Bandpass Filter using the Hanning window method is 1,163 Hz – 3,837 Hz, narrower than the Hamming window method which has a bandwidth range of 1,138 Hz – 3,862 Hz, this shows that the 20th orde filter uses Hanning window method already better than the Hamming window method, although it still does not meet the required filter specifications.

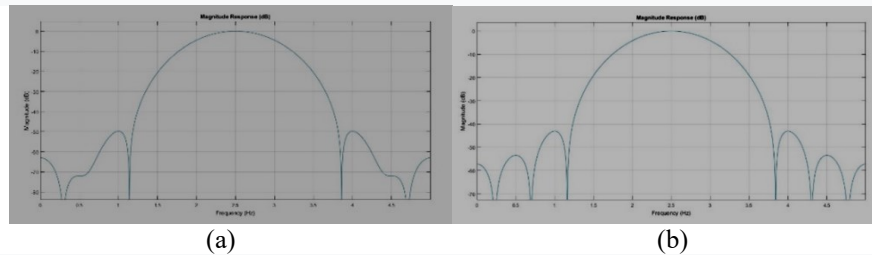


Fig. 6. Magnitude Response FIR Bandpass Digital Filter Orde 20 using (a) Hamming Window (b) Hanning Window

Fig. 7 show time domain comparison of the outputs desired signal with the actual signal filter results. The results of this simulation show that there is a delay of  $\pm 2$  seconds before the 20th orde Hamming window filter can produce an output signal. In Fig. 7(a) it is shown that the signal level of the signal output is almost close to the desired signal level while in Fig. 7(b) the signal level of the signal output is still quite far from the signal level which are desired.

Fig. 8 show time domain comparison of the outputs desired signal with the actual signal filter results. The results of this simulation show that there is a delay of  $\pm 2$  seconds before the 20th orde Hanning window filter can produce an output signal. In Fig. 8(a) it is shown that the signal level of the signal output is almost close to the desired signal level while in Fig. 8(b) the signal level of the signal output is still quite far from the signal level which are desired.

Fig. 9(a) shows a comparison of the filtered by orde 20 Hamming Window input and output signal conditions in the frequency domain. At the frequency point of 1.6 Hz, the noise signal at the input has a magnitude response value of 2533, and there is a decrease after passing through the filter to 385. Fig. 9(b) shows a comparison of the filtered by orde 20 Hanning Window input and output signal conditions in the frequency domain. At the frequency point of 1.6 Hz, the noise signal at the input has a magnitude response value of 2533, and there is a decrease after passing through the filter to 446.9 which are greater than orde 20 Hamming Window.

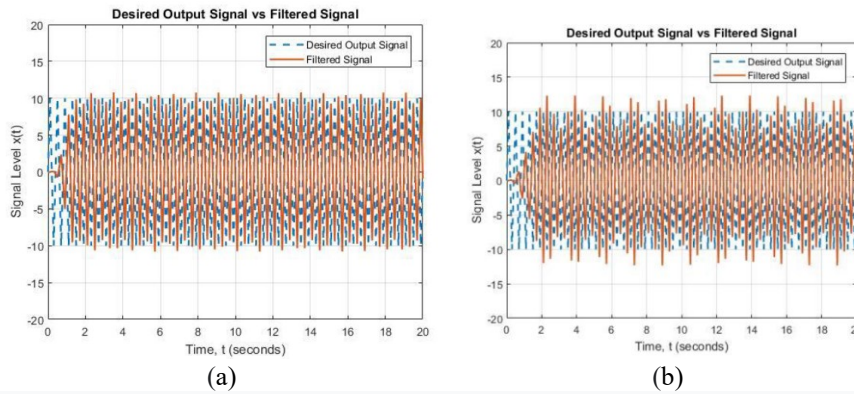


Fig. 7. Time Domain 20th Orde Filter Output Signal by Hamming Window at (a) 1.6 Hz and (b) 3.1 Hz Noise

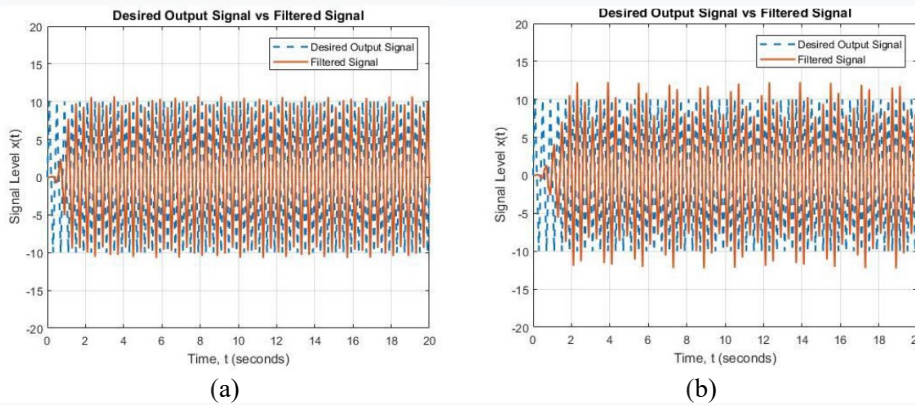


Fig. 8. Time Domain 20th Orde Filter Output Signal by Hanning Window at (a) 1.6 Hz and (b) 3.1 Hz Noise

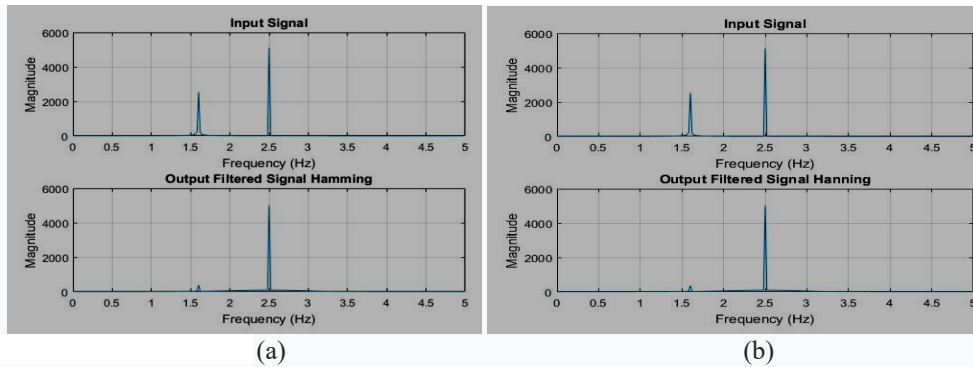
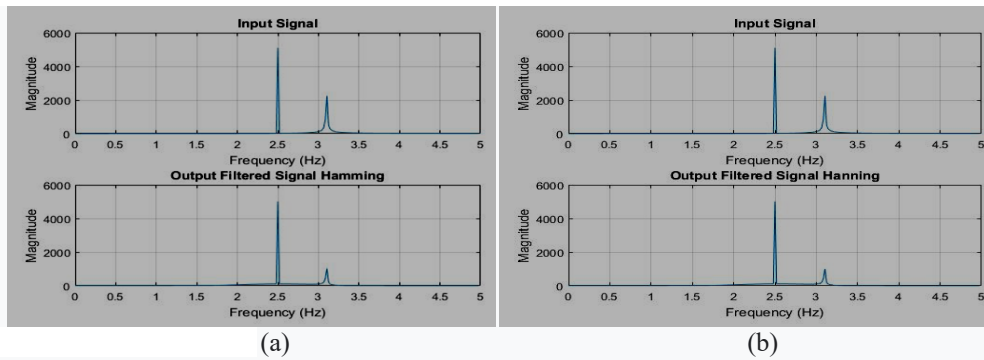


Fig. 9. Frequency Domain Output Filter Orde 20 at Noise 1.6 Hz (a) Hamming Window (b) Hanning Window

Fig. 10(a) shows a comparison of the filtered by orde 20 Hamming Window input and output signal conditions in the frequency domain. At the frequency point of 3.1 Hz, the noise signal at the input has a magnitude response value of 2246, and there is a decrease after passing through the filter to 1,019. Fig. 10(b) shows a comparison of the filtered by orde 20 Hanning Window input and output signal conditions in the frequency domain. At the frequency point of 3.1 Hz, the noise signal at the input has a magnitude response value of 2246 and there is a decrease after passing through the filter to 1084.4 which are greater than orde 20 Hamming Window.

The simulations for the FIR order 20 bandpass filter were conducted using both Hamming and Hanning Window methods. Notably, the results indicated that while the Hamming Window method failed to meet the desired bandwidth specification (2 Hz - 3 Hz), the Hanning Window method showed improvement, albeit not fully satisfying the specifications.



**Fig. 10.** Frequency Domain Output Filter Orde 20 at Noise 3.1 Hz (a) Hamming Window (b) Hanning Window

**3.4. FIR Orde 50 Digital Bandpass Filter Simulation**

FIR Orde 50 digital bandpass filter simulation using Filter Designer which is part of the MATLAB software. The filter will be simulated with 2 different methods, the Hamming Window and the Hanning Window to see which method produces the best output signal.

Fig. 11(a) indicates that the frequency bandwidth range to be passed on the orde 50 FIR digital bandpass filter using the Hamming Window method still widens to 1.642 Hz – 3.358 Hz exceeding the bandwidth range that should be 2 Hz – 3 Hz, this indicates that orde 50 Hamming Window still does not meet the required specifications. In Fig. 11(b) it is known that the frequency bandwidth range that will be passed on the 50th orde FIR Digital Bandpass Filter using the Hanning window method is 1.6653 Hz – 3.335 Hz, narrower than the Hamming window method which has a bandwidth range of 1.642 Hz – 3.358 Hz, this shows that the 50th orde filter uses Hanning window method already better than the Hamming window method, although it still does not meet the required filter specifications.

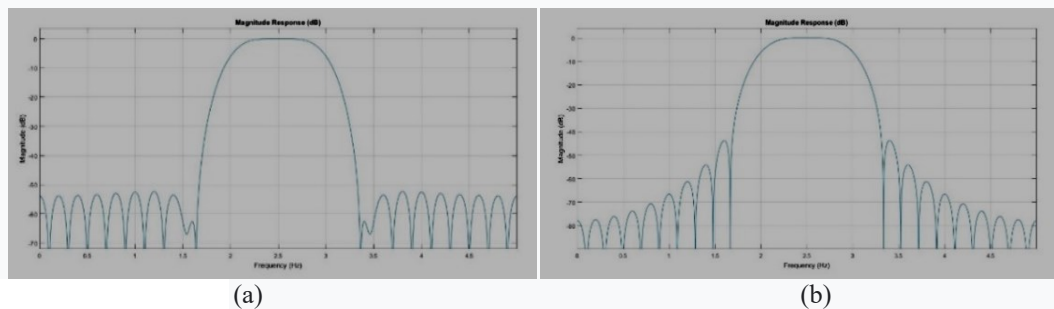


**Fig. 11.** Magnitude Response FIR Bandpass Digital Filter Orde 50 using (a) Hamming Window (b) Hanning Window

Fig. 12 show time domain comparison of the outputs desired signal with the actual signal filter results. The results of this simulation show that there is a delay of  $\pm 3$  seconds before the 50th orde Hamming window filter can produce an output signal. In Fig. 12(a) it is shown that the signal level of the signal output is the

Fig. 13 show time domain comparison of the outputs desired signal with the actual signal filter results. The results of this simulation show that there is a delay of  $\pm 3$  seconds before the 50th orde Hanning window filter can produce an output signal. In Fig. 13(a) it is shown that the signal level of the signal output is the same as the desired signal level while in Fig. 13(b) the signal level of the signal output is still not in accordance with the desired signal level, but it is already better than the signal level on the 20th orde filter.

Fig. 14(a) shows a comparison of the filtered by orde 50 Hamming Window input and output signal conditions in the frequency domain. At the frequency point of 1.6 Hz, the noise signal at the input has a magnitude response value of 2533, and there is a decrease after passing through the filter to  $\approx 0$ . Fig. 14(b) shows a comparison of the filtered by orde 50 Hanning Window input and output signal conditions in the frequency domain. At the frequency point of 1.6 Hz, the noise signal at the input has a magnitude response value of 2533, and there is a decrease after passing through the filter to  $\approx 0$ . These indicate that the noise at 1.6 Hz can be removed by using orde 50 Filter Hamming Window or orde 50 Filter Hanning Window.

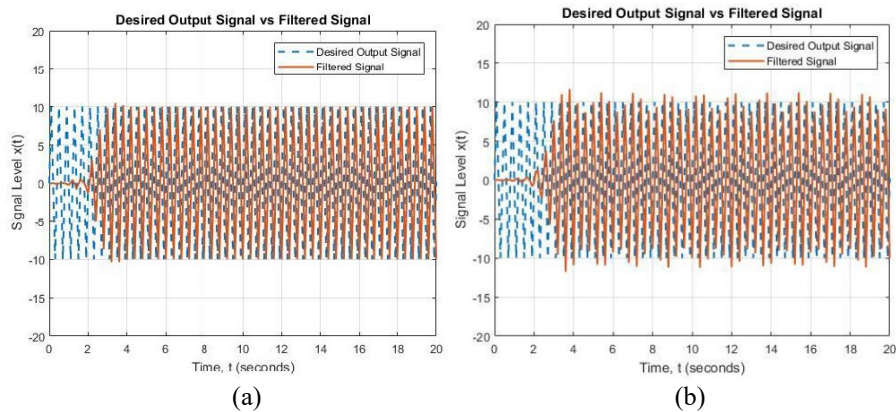


Fig. 12. Time Domain 50th Orde Filter Output Signal by Hamming Window at (a) 1.6 Hz and (b) 3.1 Hz Noise

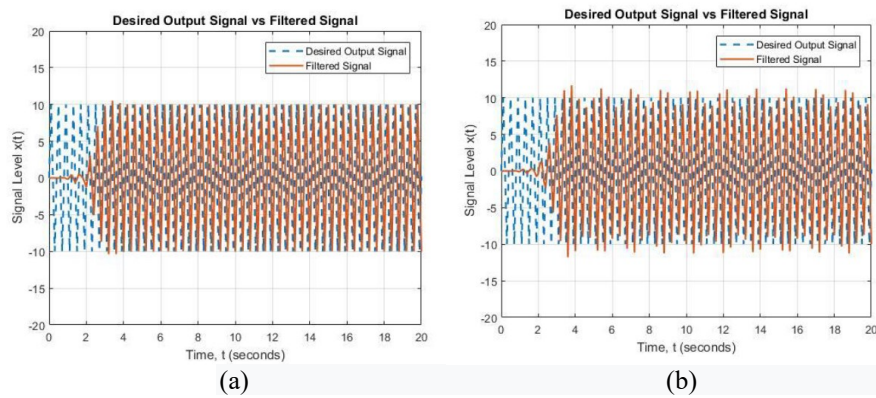


Fig. 13. Time Domain 50th Orde Filter Output Signal by Hanning Window at (a) 1.6 Hz and (b) 3.1 Hz Noise

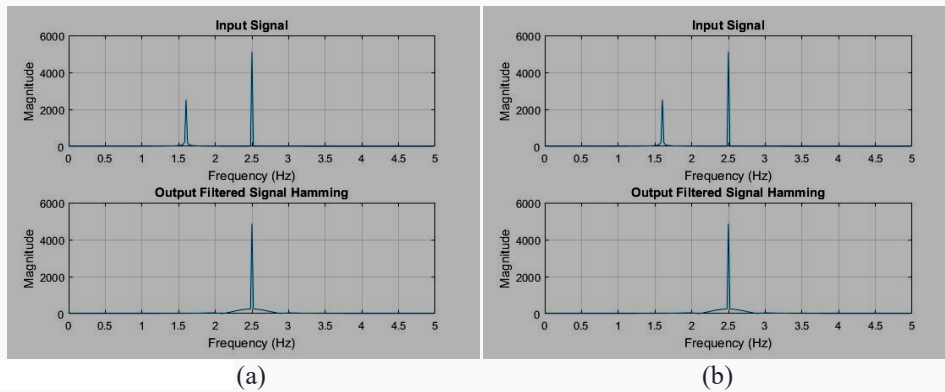
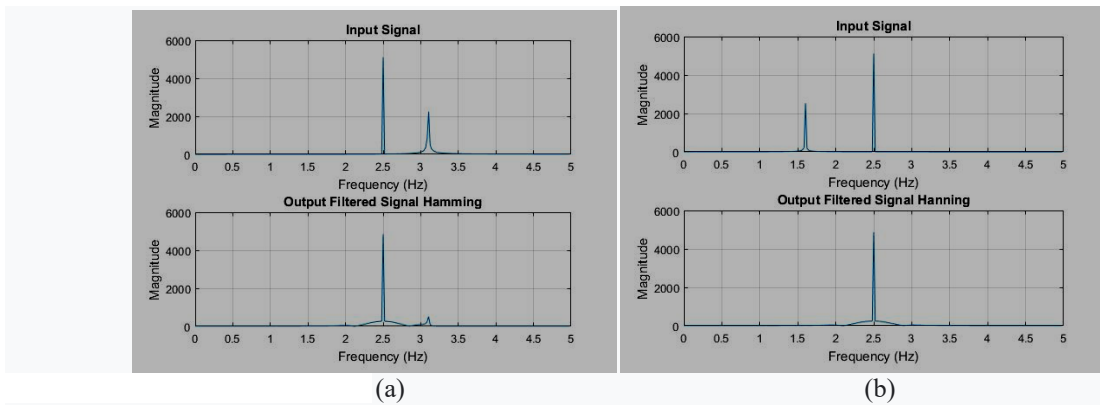


Fig. 14. Frequency Domain Output Filter Orde 50 at Noise 1.6 Hz (a) Hamming Window (b) Hanning Window

Fig. 15(a) shows a comparison of the filtered by orde 50 Hamming Window input and output signal conditions in the frequency domain. At the frequency point of 3.1 Hz, the noise signal at the input has a magnitude response value of 2246, and there is a decrease after passing through the filter to 508.4. Fig. 15(b) shows a comparison of the filtered by orde 50 Hanning Window input and output signal conditions in the frequency domain. At the frequency point of 3.1 Hz, the noise signal at the input has a magnitude response value of 2246 and there is a decrease after passing through the filter to 542.4 which are greater than orde 50 Hamming Window.



**Fig. 15.** Frequency Domain Output Filter Orde 50 at Noise 3.1 Hz (a) Hamming Window (b) Hanning Window

The FIR order 50 bandpass filter simulations, again with Hamming and Hanning Window methods, demonstrated that the Hanning Window method produced a narrower bandwidth range (1.6653 Hz - 3.335 Hz) compared to the Hamming Window method (1.642 Hz - 3.358 Hz). Although not entirely within the desired range, the Hanning Window method showcased better results.

**3.5. FIR Orde 100 Digital Bandpass Filter Simulation**

FIR Orde 100 digital bandpass filter simulation using Filter Designer which is part of the MATLAB software. The filter will be simulated with 2 different methods, the Hamming Window and the Hanning Window to see which method produces the best output signal.

In Fig. 16(a), it is known that the range of frequency bandwidth that will be passed on the 100th order FIR Digital Bandpass Filter using the Hamming window method is 1.827 Hz – 3.173 Hz which is almost equal to the required bandwidth specification is 2 Hz – 3 Hz, this shows that the 100th order filter has a better bandwidth range than the 20th and 50th orde filters. In Fig. 16(b), it is known that the frequency bandwidth range that will be passed to the 100th order FIR digital bandpass filter using the Hanning window method is 1,833 Hz – 3,167 Hz, narrower than the Hamming window method which has a bandwidth range of 1,827 Hz – 3,173 Hz, this shows that the 100th order filter uses the Hanning window method is better than the Hamming window method.

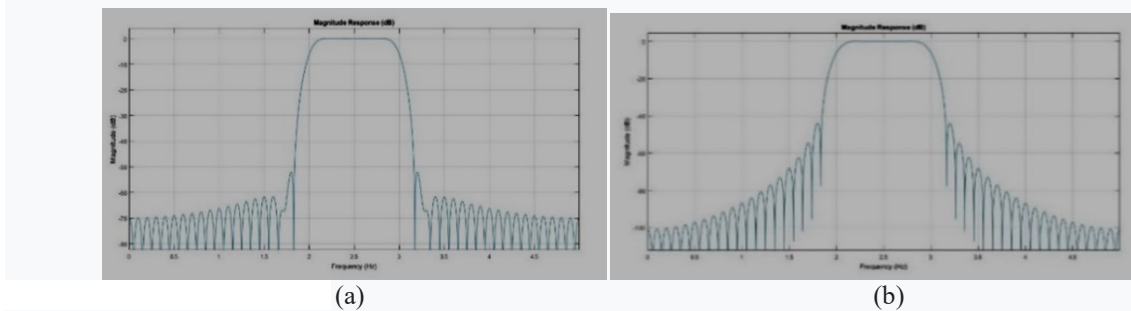


**Fig. 16.** Magnitude Response FIR Bandpass Digital Filter Orde 100 using (a) Hamming Window (b) Hanning Window

Fig. 17 show time domain comparison of the outputs desired signal with the actual signal filter results. The results of this simulation show that there is a delay of  $\pm 6$  seconds before the 100th orde Hamming window filter can produce an output signal. In Fig. 17(a) it is shown that the signal level of the signal output is the same as the desired signal level while in Fig. 17(b) signal level from the signal output is almost the same as the desired signal level.

Fig. 18 show time domain comparison of the outputs desired signal with the actual signal filter results. The results of this simulation show that there is a delay of  $\pm 6$  seconds before the 100th orde Hanning window filter can produce an output signal. In Fig. 18(a) it is shown that the signal level of the signal output is the same as the desired signal level while in Fig. 18(b) signal level from the signal output is almost the same as the desired signal level.

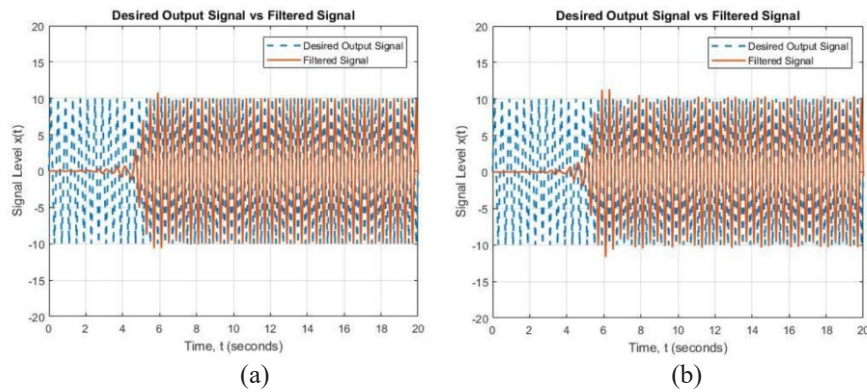


Fig. 17. Time Domain 100th Orde Filter Output Signal by Hamming Window at (a) 1.6 Hz and (b) 3.1 Hz Noise

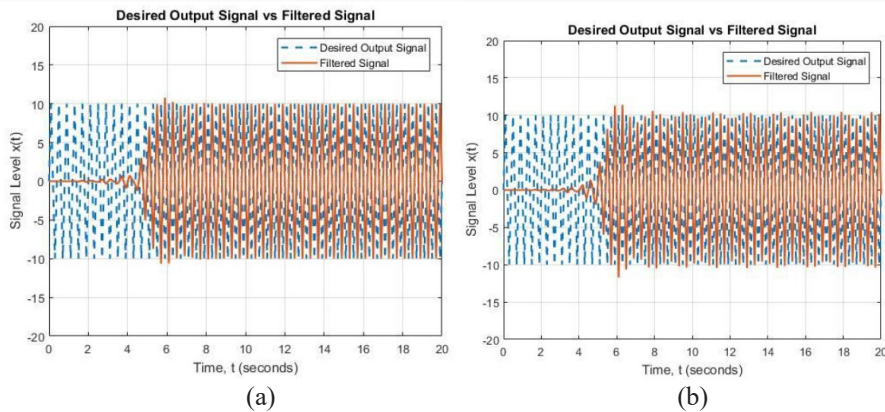


Fig. 18. Time Domain 100th Orde Filter Output Signal by Hanning Window at (a) 1.6 Hz and (b) 3.1 Hz Noise

Fig. 19(a) shows a comparison of the filtered by orde 100 Hamming Window input and output signal conditions in the frequency domain. At the frequency point of 1.6 Hz, the noise signal at the input has a magnitude response value of 2533, and there is a decrease after passing through the filter to  $\approx 0$ . Fig. 14(b) shows a comparison of the filtered by orde 100 Hanning Window input and output signal conditions in the frequency domain. At the frequency point of 1.6 Hz, the noise signal at the input has a magnitude response value of 2533, and there is a decrease after passing through the filter to  $\approx 0$ . These indicate that the noise at 1.6 Hz can be removed by using orde 50 Filter Hamming Window or orde 50 Filter Hanning Window.

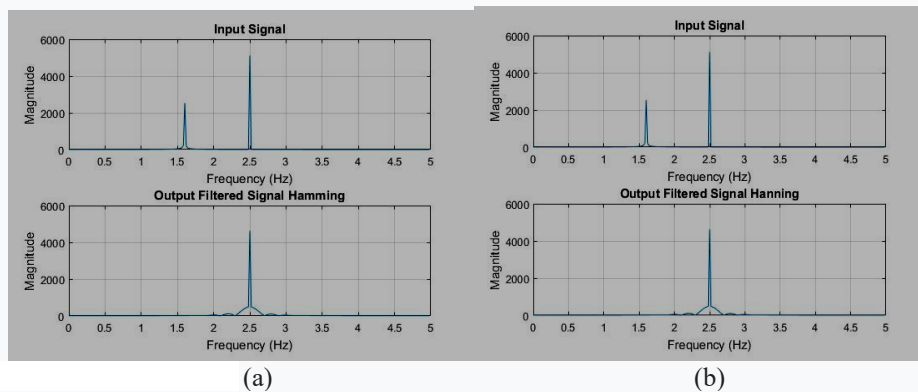
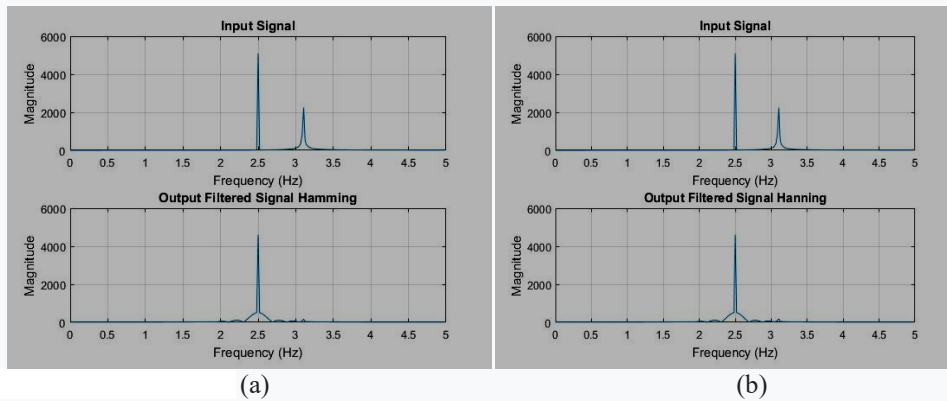


Fig. 19. Frequency Domain Output Filter Orde 100 at Noise 1.6 Hz (a) Hamming Window (b) Hanning Window

Fig. 20(a) shows a comparison of the filtered by orde 100 Hamming Window input and output signal conditions in the frequency domain. At the frequency point of 3.1 Hz, the noise signal at the input has a magnitude response value of 2246, and there is a decrease after passing through the filter to 167.7. Fig. 15(b) shows a comparison of the filtered by orde 100 Hanning Window input and output signal conditions in the frequency domain. At the frequency point of 3.1 Hz, the noise signal at the input has a magnitude response value of 2246 and there is a decrease after passing through the filter to 195.4 which are greater than orde 100 Hamming Window.



**Fig. 20** Frequency Domain Output Filter Orde 100 at Noise 3.1 Hz (a) Hamming Window (b) Hanning Window

For the FIR order 100 bandpass filter, both Hamming and Hanning Window methods yielded narrower bandwidth ranges (1.827 Hz - 3.173 Hz and 1.833 Hz - 3.167 Hz, respectively) that approached the desired specification (2 Hz - 3 Hz). Particularly, the Hanning Window method demonstrated superior performance in achieving a closer match to the required bandwidth.

### 3.6. Time and Frequency Domain Analysis

Time domain analysis illustrated the signal output behavior of the filters, highlighting the trade-off between signal delay and accuracy. Both the Hamming and Hanning Window methods exhibited signal delays of  $\pm 2$  to  $\pm 6$  seconds, with signal levels approaching the desired levels, albeit not consistently. Frequency domain analysis provided insight into how the filters affected the noise signals. Notably, the filters using the Hanning Window method generally demonstrated better noise reduction at specific frequencies compared to the Hamming Window method.

### 3.7. Overall Assessment

While none of the simulated filters fully met all specifications, the FIR order 100 bandpass filter with the Hanning Window method exhibited the most promising results, achieving a bandwidth range that closely aligned with the desired specification. However, further optimization and refinement might be required to achieve more precise filtering for fetal Doppler applications.

## 4. CONCLUSION

In this study, we conducted a comprehensive investigation into the design and performance of FIR filters using different window methods and orders for processing fetal Doppler signals. Our analysis yielded valuable insights into the efficacy of these filters in enhancing the clarity and accuracy of fetal heartbeat detection. From our experimental results, several key findings emerged:

**Frequency Bandwidth Range:** Among the tested filters, the Orde 100 Hanning Window filter demonstrated the most promising frequency bandwidth range, spanning from 1.833 Hz to 3.167 Hz. This suggests that the Hanning Window approach is effective in isolating the desired fetal heartbeat frequencies.

**Signal Delay:** The Orde 20 filters, both Hamming and Hanning, exhibited the shortest delays of  $\pm 2$  seconds, while the Orde 100 filters, employing both window methods, showed longer delays of  $\pm 6$  seconds. These delay values are crucial considerations for real-time fetal monitoring applications.

**Time Domain Output Desired Signal:** For the noise frequency of 1.6 Hz, both Orde 100 Hamming and Orde 100 Hanning filters produced signal outputs closely matching the desired signal level. Similarly, for the

noise at 3.1 Hz, the signal output level was nearly aligned with the desired level, indicating effective noise reduction.

Frequency Domain Output: Notably, the Orde 100 Hamming filter exhibited superior performance in the frequency domain. It significantly attenuated the noise signal at both 1.6 Hz and 3.1 Hz frequencies, reducing the magnitude response values to near-zero and 167.7, respectively.

Based on our findings, we recommend further exploration to refine and optimize the filtering process for fetal Doppler signal analysis. Specifically, we propose investigating higher-order filters, such as Orde 150 and Orde 200, to determine if enhanced filtering capabilities can be achieved. These higher-order filters might provide even better noise reduction and signal enhancement, contributing to more accurate fetal health assessments.

In conclusion, this study sheds light on the potential of FIR filters, especially the Orde 100 Hanning filter, for improving fetal Doppler signal processing. By fine-tuning parameters and exploring more advanced filter designs, we anticipate that our research will contribute to the advancement of fetal monitoring techniques and potentially lead to enhanced maternal and fetal healthcare outcomes.

## REFERENCES

- [1] P. Hamelmann, M. Mischi, A. F. Kolen, J. O. E. H. van Laar, R. Vullings, and J. W. M. Bergmans, "Fetal Heart Rate Monitoring Implemented by Dynamic Adaptation of Transmission Power of a Flexible Ultrasound Transducer Array," *Sensors*, vol. 19, no. 5, pp. 1195-1215, 2019, <https://doi.org/10.3390/s19051195>.
- [2] P. Hamelmann, R. Vullings, A. F. Kolen, J. W. M. Bergmans, J. O. E. H. van Laar, P. Tortoli, and M. Mischi, "Doppler Ultrasound Technology for Fetal Heart Rate Monitoring: a Review," *IEEE Transactions on Ultrasonic, Ferroelectrics, and Frequency Control*, vol. 67, no. 2, pp. 226 – 238, 2020, <https://doi.org/10.1109/tuffc.2019.2943626>.
- [3] T. Kupka, A. Matonia, M. Jezewski, J. Jezewski, K. Horoba, J. Wrobel, R. Czabanski, and R. Martinek, "New Method for Beat-to-Beat Fetal Heart Rate Measurement Using Doppler Ultrasound Signal," *Sensors*, vol. 20, no. 15, 2020, <https://doi.org/10.3390/s20154079>.
- [4] J. Vargas-Calixto, P. Warrick, and R. Kearney, "Estimation and Discriminability of Doppler Ultrasound Fetal Heart Rate Variability Measures," *Frontiers in Artificial Intelligence*, vol. 4, 2021, <https://doi.org/10.3389/frai.2021.674238>.
- [5] S. A. Alnuaimi, S. Jimaa, and A. H. Khandoker, "Fetal Cardiac Doppler Signal Processing Techniques: Challenges and Future Research Directions," *Frontiers in Bioengineering and Biotechnology*, vol. 5, 2017, <https://doi.org/10.3389/fbioe.2017.00082>.
- [6] P. F. Mdoe, H. L. Ersdal, E. R. Mduma, J. M. Perlman, R. Moshiri, P.T. Wangwe, and H. Kidanto, "Intermittent fetal heart rate monitoring using a fetoscope or hand held Doppler in rural Tanzania: a randomized controlled trial," *BMC Pregnancy and Childbirth*, vol. 18, 2018, <https://doi.org/10.1186/s12884-018-1746-9>.
- [7] S. P. von Steinburg, A. L. Boulesteix, C. Lederer, S. Grunow, S. Schiermeier, W. Hatzmann, K. T. M. Schneider, and M. Daumer, "What is the "normal" fetal heart rate?," *Peer J*, vol. 1, p. e82, 2013, <https://peerj.com/articles/82/>.
- [8] T. Ghi, E. Di Pasquo, A. Dall'Asta, A. Commare, E. Melandri, A. Casciaro, S. Fieni, and T. Frusca, "Intrapartum fetal heart rate between 150 and 160 bpm at or after 40 weeks and labor outcome," *Acta Obstetrica et Gynecologica Scandinavica*, vol. 100, no. 3, 2021, <https://doi.org/10.1111/aogs.14024>.
- [9] O. Sylwestrzak, A. Nowakowska, J. Murlewska, and M. Respondek-Liberska, "Normal ranges of fetal heart rate values for healthy fetuses in Poland, as determined by ultrasound between weeks 18 and 29 of gestation," *Kardiologia Polska*, vol. 79, no. 11, pp. 1245-1250, 2021, <https://doi.org/10.33963/kp.a2021.0119>.
- [10] P. Anastasiadis, P. A. Anninos, M. V. Ludinghausen, A. Kotini, G. Galazios, and B. Limberis, "Fetal Magnetocardiogram Recordings and Fourier Spectral Analysis," *Journal of Obstetrics and Gynaecology*, vol. 19, no. 4, pp. 390 – 393, 1999, <https://doi.org/10.1080/01443619964715>.
- [11] M. Tarvonen, P. Hovi, S. Sainio, P. Vuorela, S. Andersson, and K. Teramo, "Intrapartum zigzag pattern of fetal heart rate is an early sign of fetal hypoxia: A large obstetric retrospective cohort study," *Acta Obstetrica et Gynecologica Scandinavica*, vol. 100, no. 2, 2021, <https://doi.org/10.1111/aogs.14007>.
- [12] L. Heelan, "Fetal Monitoring: Creating a Culture of Safety with Informed Choice", *The Journal of Perinatal Education*, vol. 22, no. 3, pp. 156 – 165, 2013, <https://doi.org/10.1891/1058-1243.22.3.156>.
- [13] E. W. Abdulhay, R. J. Oweis, A. M. Alhaddad, F. N. Sublaban, M. A. Radwan, and H. M. Almasaeed, "Review Article: Non-Invasive Fetal Heart Rate Monitoring Techniques," *Biomedical Science and Engineering*, vol. 2, no. 3, pp. 53 – 67, 2014, [12691/bse-2-3-2](https://doi.org/10.12691/bse-2-3-2).
- [14] M. Peters, J. Crowe, J. F. Piéri, H. Quartero, B. Hayes-Gill, D. James, J. Stinstra, and S. Shakespeare, "Monitoring the fetal heart non-invasively: a review of methods," *Journal of Perinatal Medicine*, vol. 29, no. 5, pp. 408-416, 2001, <https://doi.org/10.1515/jpm.2001.057>.
- [15] G. Aggarwal and Y. Wei, "Non-Invasive Fetal Electrocardiogram Monitoring Techniques: Potential and Future Research Opportunities in Smart Textiles," *Signals*, vol. 2, no. 3, pp. 392-412, 2021, <https://doi.org/10.3390/signals2030025>.

- [16] P. Das and M. Karmakar, "A New Window Function to Design FIR Filter with an Improved Frequency Response for Suppressing Side-Lobe Attenuation and Study Comparison with the Other Windows," *International Journal of Engineering Research & Technology (IJERT)*, vol. 2, no. 12, pp. 314-321, 2013, <https://www.ijert.org/research/a-new-window-function-to-design-fir-filter-with-an-improved-frequency-response-for-suppressing-side-lobe-attenuation-and-study-comparison-with-the-other-windows-IJERTV2IS120211.pdf>.
- [17] P. Podder, T. Z. Khan, M. H. Khan, and M. M. Rahman, "Comparative Performance Analysis of Hamming, Hanning and Blackman Window," *International Journal of Computer Applications*, vol. 96, no. 18, pp. 1-7, 2014, <https://doi.org/10.5120/16891-6927>.
- [18] K. R. Rani and R. Baskar, "FIR Digital Filter Designed by using Hamming and Hanning (Windows) Method," *International Journal of Pure and Applied Mathematics*, vol. 119, no. 18, pp. 1565 – 1576, 2018, <https://acadpubl.eu/hub/2018-119-18/2/128.pdf>.
- [19] M. Mynuddin, M. Tanjimuddin, M. M. Rana, and Abdullah, "Designing a Low-Pass FIR Digital Filter by Using Hamming Window and Blackman Window Technique," *Science Journal of Circuits, Systems and Signal Processing*, vol. 4, no. 2, pp. 9 – 13, 2015, <http://dx.doi.org/10.11648/j.cssp.20150402.11>.
- [20] D. J. Jwo, I. H. Wu, and Y. Chang, "Windowing Design and Performance Assessment for Mitigation of Spectrum Leakage," *International Symposium on Global Navigation Satellite System*, vol. 94, 2019, <https://doi.org/10.1051/e3sconf/20199403001>.
- [21] K. Avci, "Design of FIR Filters using Exponential - Hamming Window Family," *Turkish Journal of Electrical Engineering & Computer Sciences*, vol. 24, pp. 2513 – 2524, 2016, <https://doi.org/10.3906/elk-1312-246>.
- [22] G. Gautam, "Spectral Analysis of Rectangular, Hanning, Hamming and Kaiser Window for Digital FIR Filter," *International Journal of Smart Convergence*, vol. 4, no. 2, pp. 138-144, 2015, <http://dx.doi.org/10.7236/IJASC.2015.4.2.138>.
- [23] M. S. Mandloi and G. R. Kumrey, "FIR High pass Filter for Improving performance Characteristics of Various Windows," *International Journal of Advanced Engineering Research and Science (IJAERS)*, vol. 4, no. 1, 2017, <http://dx.doi.org/10.22161/ijaers.4.1.15>.
- [24] A. T. Seed, Z. R. Saber, A. M. Sana, and M. A. Hameed, "Eliminating Unwanted Signals in Sound by using Digital Signal Processing System," *Indonesian Journal of Electrical Engineering and Computer Science*, vol. 18, no. 2, pp. 829 – 834, 2020, <http://doi.org/10.11591/ijeecs.v18.i2.pp829-834>.
- [25] R. Martinek, M. Ladrova, M. Sidikova, R. Jaros, K. Behbehani, R. Kahankova, and A. Kawala-Sterniuk, "Advanced Bioelectrical Signal Processing Methods: Past, Present, and Future Approach—Part III: Other Biosignals," *Sensor*, vol. 21, no. 18, pp. 6064-6095, 2021, <https://doi.org/10.3390/s21186064>.
- [26] M. Boyer, L. Bouyer, J. S. Roy, and A. Campeau-Lecours, "Reducing Noise, Artifacts and Interference in Single-Channel EMG Signals: A Review," *Sensor*, vol. 23, no. 6, pp. 2927-2955, 2023, <https://doi.org/10.3390/s23062927>.
- [27] A. Cheveigne and I. Nelken, "Filters: When, Why, and How (Not) to Use Them," *Neuron*, vol. 102, no. 2, pp. 280-293, 2019, <https://doi.org/10.1016/j.neuron.2019.02.039>.
- [28] A. V. Belov, A. A. Anisimov, T. V. Sergeev, and N. B. Suvorov, "Tunable band-pass filter for continuous spectral analysis of cardiointervalogram," *Journal of Physics: Conference Series*, vol. 1515, 2020, <https://doi.org/10.1088/1742-6596/1515/5/052064>.
- [29] S. Koshita, Y. Kumamoto, M. Abe, and M. Kawamata, "High-order center-frequency adaptive filters using block-diagram-based frequency transformation," *Conference: Proceedings of the IEEE International Conference on Acoustics, Speech, and Signal Processing, ICASSP*, pp. 4284-4287, 2011, <http://dx.doi.org/10.1109/ICASSP.2011.5947300>.
- [30] T. Singh and H. S. Josan, "Design of Low Pass Digital FIR Filter Using Cuckoo Search Algorithm," *International Journal of Engineering Research and Applications*, vol. 4, no. 8, pp. 72-77, 2014, [https://www.ijera.com/papers/Vol4\\_issue8/Version%204/L48047277.pdf](https://www.ijera.com/papers/Vol4_issue8/Version%204/L48047277.pdf).
- [31] S. Zahoor and S. Naseem, "Design and implementation of an efficient FIR digital filter," *Cogent Engineering*, vol. 4, no. 1, 2017, <https://doi.org/10.1080/23311916.2017.1323373>.
- [32] D. J. Jwo, W. Y. Chang, and I. H. Wu, "Windowing Techniques, the Welch Method for Improvement of Power Spectrum Estimation," *Computers, Materials & Continua*, vol. 67, no. 3, pp. 3983-4003, 2021, <https://doi.org/10.32604/cmc.2021.014752>.
- [33] R. Sivarajan and B. Elango, "A Novel Window Function for Designing FIR Low Pass and Band Pass Filter," *International Journal of Science and Research (IJSR)*, vol. 4, no. 9, 2015, <https://www.ijer.net/archive/v4i9/SUB158475.pdf>.
- [34] D. Maillet, C. Zacharie, and B. Rémy, "Identification of an impulse response through a model of ARX structure," *Journal of Physics: Conference Series*, vol. 2444, 2023, <https://doi.org/10.1088/1742-6596/2444/1/012002>.
- [35] S. Dogra and N. Sharma, "Comparison of Different Techniques to Design of Filter," *International Journal of Computer Applications*, vol. 97, no. 1, pp. 25 – 29, 2014, <https://doi.org/10.5120/16972-6823>.
- [36] S. Chandra, S. Bhowmik, S. Bhaumik, and S. Malik, "A comparative study on Main and Side lobe of Frequency response curve for FIR Filter using Frequency Series Expansion Method," *IOSR Journal of Electronics and Communication Engineering (IOSR-JECE)*, vol. 10, no. 2, pp. 79-82, 2015, <https://doi.org/10.9790/2834-10237982>.
- [37] S. N. Sharma, R. Saxena, and S. C. Saxena, "Sharpening the response of an FIR filter using fractional Fourier transform," *Journal of the Indian Institute of Science*, vol. 86, no. 2, pp. 163-168, 2006, <https://journal.iisc.ac.in/index.php/iisc/article/view/2290>.

- [38] V. Vaishali and M.K. Singh, "Comparative Study of Digital FIR Filter (Using Various Windows) on DSP Processor," *International Research Journal of Engineering and Technology (IRJET)*, vol. 07, no. 08, pp. 3951-3956, 2020, <https://www.irjet.net/archives/V7/i8/IRJET-V7I8680.pdf>.
- [39] M. Kaur and S.P. Kaur, "FIR Low Pass Filter Designing Using Different Window Functions and their Comparison using MATLAB," *International Journal of Advanced Research in Electrical, Electronics and Instrumentation Engineering*, vol. 5, no. 2, pp. 753-758, 2016, [https://www.ijareeie.com/upload/2016/february/16\\_FIR.pdf](https://www.ijareeie.com/upload/2016/february/16_FIR.pdf).
- [40] V. O. Mmeremikwu, "Digital Filter Enhancement of Electrocardiographic Signal Using Parzen Window," *World Journal of Innovative Research (WJIR)*, vol. 4, no. 5, pp. 1-4, 2018, [https://www.wjir.org/download\\_data/WJIR0405015.pdf](https://www.wjir.org/download_data/WJIR0405015.pdf).
- [41] J. Zhao, "Modeling and Simulation of Digital Filter," *4th National Conference on Electrical, Electronics and Computer Engineering (NCEECE)*, pp. 1333-1338, 2015, <https://www.atlantis-pess.com/proceedings/ncece-15/25847103>.
- [42] S. Srivastava and E. R. Mehra, "Design and Analysis of Band Pass FIR Filter Using Different Window Techniques," *International Journal of Engineering Research & Technology (IJERT)*, vol. 3, no. 2, pp. 506-511, 2014, <https://www.ijert.org/design-and-analysis-of-band-pass-fir-filter-using-different-window-techniques>.
- [43] R. Patel, E.M. Kumar, A.K. Jaiswal, and E.R. Saxena, "Design Technique of Bandpass FIR filter using Various Window Function," *IOSR Journal of Electronics and Communication Engineering (IOSR-JECE)*, vol. 6, no. 6, pp. 52-57, 2013, <https://www.iosrjournals.org/iosr-jece/papers/Vol6-Issue6/10665257.pdf>.
- [44] S. Pandey, S. Choudhary, P. K. Rahi, "Design of Low Pass Fir Filter Using Rectangular, Bartlett and Blackman-Harris Window Techniques," *International Journal of Advanced Research in Computer and Communication Engineering*, vol. 6, no. 3, pp. 434-441, 2017, <https://doi.org/10.17148/IJARCCE.2017.63100>.
- [45] R. P. Narwaria, M. Kumar, "Comparison of FIR Filter Using Different Window Functions," *International Research Journal of Engineering and Technology (IRJET)*, vol. 05, no. 10, pp. 634-637, 2018, <https://www.irjet.net/archives/V5/i10/IRJET-V5I10118.pdf>.
- [46] M. G. Beaty and M. Dogson, "An Application of a General Sampling Theorem," *Results in Mathematics*, vol. 34, pp. 241-254, 1998, <https://doi.org/10.1007/BF03322054>.
- [47] H. D. Luke, "The Origins of the Sampling Theorem," *IEEE Communications Magazine*, pp. 106-108, 1999, <https://doi.org/10.1109/35.755459>.

## BIOGRAPHY OF AUTHORS



**Hartono Siswono**, Head of Graduate Program in Electrical Engineering at Gunadarma University. Graduated from Indiana Institute of Technology, Indiana, USA in January 1988, With the degree of Bachelor of Science in Engineering. In July 2000, graduated with the degree of Master of Science in Electrical Engineering from University of Indonesia. Got the Doctoral degree in Electrical Engineering from University of Indonesia in January 2006. Started as an instructor in University of Gunadarma since 1993, and since June 2013 as Head of Electrical Engineering Department University of Gunadarma. Since March 2022 as Head of Graduate Program in Electrical Engineering in University of Gunadarma. When studying in the United States of America, also work as an assistant for Electrical Engineering Department Indiana Institute of Technology, and also as the President of Indonesian Students Association in the United States of America for two periods. Also as an author of six books, which are: "Digital System Design by using XILINX (Perancangan Sistem Digital Simulator XILINX)", "Signal Processing System (Sistem Pemrosesan Sinyal)", "Control System (Dasar Sistem Kontrol)", "Digital Signal Processing (Pengolahan Sinyal Digital)", "Linear System Analysis and Theory (Teori dan Analisis Sistem Linier), and "Analog Filter Design (Perancangan Filter Analog)". Email: [hartono@staff.gunadarma.ac.id](mailto:hartono@staff.gunadarma.ac.id). ORCID: <http://orcid.org/0000-0001-8700-7667>. GOOGLE SCHOLAR ID: PaoQBtwAAAAJ&hl. SCOPUS ID: 35796100200.



**Widayastuti**, Graduated from Gunadarma University, Indonesia, in March 2010, with the degree of Bachelor of Electro Engineering. In July 2000, graduated with the degree of Master Electrical Engineering from Gunadarma University. Started as an instructor in University of Gunadarma since 2013. Also work as staff of Electro laboratory in Gunadarma University since 2014. Since September 2019 is studying in Doctoral Program in University of Gunadarma.



**Yohanes Dovan**, Graduated from Gunadarma University, Indonesia, in September 2020, with the degree of Bachelor of Electro Engineering. Also work as staff of Electro laboratory in Gunadarma University since 2020.



**Dyah Nur'ainingsih**, Graduated from Gunadarma University, Indonesia, in 1999 with the degree of Bachelor of Electro Engineering. In 2002 graduated with the degree of Master Electrical Engineering from Gunadarma University. Graduated with doctoral degree from University of Gunadarma in 2016. Since 2006 as a Vice Head of Electrical engineering Laboratory in University of Gunadarma.